Three-Dimensional Flow in Transonic Axial Compressor Blade Rows[1]

J. E. McCune

Massachusetts Institute of Technology

Olufemi Okurounmu

University of Lagos
Lagos, Nigeria

Recent developments in the three-dimensional aerodynamic theory of inviscid flow in transonic axial compressors are reviewed briefly. Emphasis is placed on the newly completed lifting surface theory of a transonic ducted rotor. The relationship between the lifting surface theory and axisymmetric through-flow theories of turbomachines is illustrated; a few examples of the additional information obtainable from the new theory are then given. Quasi-two-dimensional cascade theory can also be extracted from the present analysis and the relevance of cascade theory to the actual three-dimensional problem assessed. Details are reported elsewhere, but some of the qualitative conclusions are discussed here. Even moderate departure from uniform spanwise loading of the rotor blades, for example, leads to a rather profound influence of the downstream wakes, suggesting the need for considerable care in applying cascade data on a direct quasi-two-dimensional basis.

The inviscid, three-dimensional, compressible flow through an axial compressor rotor or ducted fan can be described in terms of the perturbation of the incoming flow by the rotor and its wake. If the incoming flow is sufficiently uniform and regular, and if stator interference can be neglected as a first approximation, then the flow is steady in coordinates fixed in the rotor. If, moreover, the perturbations induced by the rotor are "small" they can be described by a velocity potential which satisfies the convected wave equation.

[1] A major part of this work was supported by the United Aircraft Corporation Research Laboratories while Dr. Okurounmu was a member of the Research Staff at that Laboratory. A portion of the work of J. E. McCune was also supported by the Pratt and Whitney Division of United Aircraft Corporation.

For steady flow in rotor coordinates, when the relative Mach number is everywhere small, the governing equation for the velocity potential reduces to Laplace's equation. In this paper, however, we will be concerned with transonic rotors (i.e., rotors operating with subsonic axial Mach numbers), while the relative Mach numbers at the tip may be supersonic. The relative Mach number at the hub is usually subsonic and, therefore, the flow will generally be of a mixed type. The governing (linear) equation changes from elliptic to hyperbolic type at the "sonic cylinder," $r=r_s$, where $\omega^2 r_s^2+U^2=a^2$. Because of three-dimensional effects, however, the linear theory does not exhibit the degeneracy for relative Mach numbers approaching unity which occurs in two-dimensional theory.

The coordinate system we use in this paper is fixed in the rotor (fig. 1); ω is the angular velocity of the rotor, U the (purely axial) velocity far upstream, a the (undisturbed) speed of sound and r the radius; x is the axial coordinate, θ the azimuthal. The corresponding dimensionless variables are $(z,\theta,\sigma)\equiv(\omega x/U,\theta,\omega r/U)$.

In this paper we will be concerned primarily with the lifting problem. The thickness problem was treated earlier (see refs. 1 and 2). In those papers, source-type singular solutions (B radial source "spikes", where B is the number of blades in the rotor) were constructed by superposition of the acoustic eigenmodes of the system in a straight annular duct of infinite extent. These source spikes, of arbitrary strength, $Q(r)$, were then

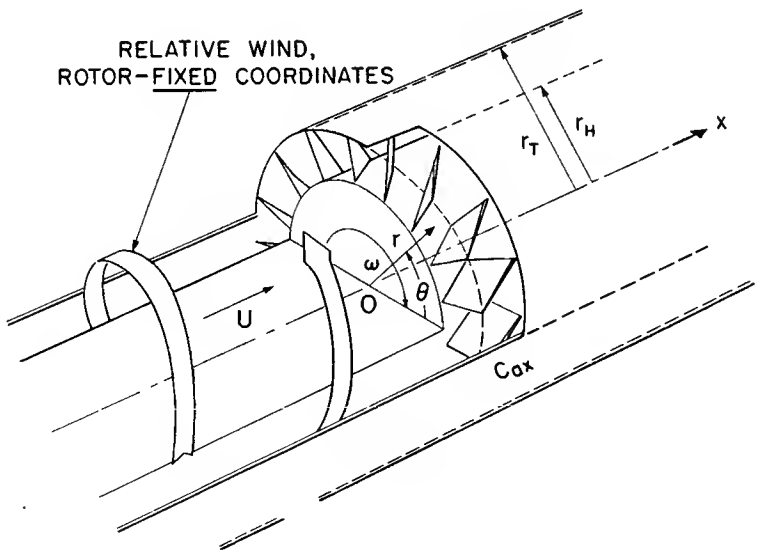

FIGURE 1.—*Geometry and coordinate system fixed in rotor. ω is the angular speed of the rotor relative to the shroud.*

distributed over helical surfaces of finite chord approximating the blades, thus representing blades of arbitrary thickness distribution (with the limitation, of course, that the thickness-to-chord ratio remain small). The camber line of the blades was left free in that study so that the "rotor" produced no lift and hence no positive work. Attention was thus focused on the effects of blade thickness in three dimensions.

The conditions under which quasi-two-dimensional cascade theory could be recovered from the three-dimensional theory were delineated in reference 1, while it was shown in reference 2 that large departures from quasi-two-dimensionality are to be expected in the transonic regime because of an acoustic resonance of certain eigenmodes. It was also shown that the wave drag due to thickness should be considerably smaller than that corresponding to quasi-two-dimensional (strip) theory.

Reference 3 describes experiments on a "free-wheeling" transonic rotor undertaken in part to verify the latter theoretical result. In this regard, the experiment was somewhat inconclusive, partly due to the difficulty of identifying and separating out the various types of drag and/or losses and partly due to the fact that any actual (rigid) rotor, of course, produces lift, varying from hub to tip. For a free-wheeling rotor (zero torque input) the result is that vorticity is shed downstream, adding substantially to the drag.

In order to complete the three-dimensional potential theory, the basis elements of the theoretical *lifting problem* were set up in reference 3. Following the general procedure of superposing the appropriate eigenmodes to construct singular (Green's function) solutions, B bound *vortex* spikes were constructed, having arbitrary strength $\Gamma(r)$. (The method is almost identical to that used in ref. 4, except that a finite hub-to-tip ratio was included and an important error occurring in ref. 4 was removed.)

The most important new feature of the lifting problem, relative to the thickness problem, is the necessity of including the downstream wakes of shed vorticity (one helical wake for each blade) with strength proportional to $d\Gamma/dr$, the rate of change of bound circulation along the span. This is done by a slight modification of the method of Reissner (ref. 5), to allow for the presence of the hub and shroud. Thus, a "wake potential" is included in the downstream flow, added to the acoustic eigenmodes, and construction of the bound vortices at the blades proceeds as before, with the wakes now included. It is interesting to observe that the wakes themselves excite acoustic modes, except when $\Gamma(r) = \text{constant}$.

The acoustic eigenmodes mentioned above are versions of the familiar "spinning" modes associated with cylindrical geometry (refs. 6 and 7). If the relative Mach number at the tip exceeds unity, some of these modes propagate undiminished in strength (in the inviscid, linear theory) upstream and downstream, while the remaining modes die out exponentially at large distances from the rotor. The propagating modes are said

to be above "cut-off"; modes near cut-off can set up the acoustic resonances mentioned above. One effect of such resonances is to create a significant spanwise flow, yielding strong communication between hub and tip. Under these conditions (which require supersonic tip Mach numbers), a *hub* section with a subsonic relative Mach number can nevertheless have a pressure distribution over the blade which is more typical of supersonic flow than subsonic flow (refs. 1, 2, and 8).

In reference 9, the lifting theory was refined and extended. In that paper, the blades were characterized by their total bound vorticity, $\Gamma(r)$, and the first-order static pressure rise across the rotor, the turning angles, the torque required, etc., were determined as functions of Γ. For example, the first-order static pressure rise was found to be

$$C_{p_\infty} \equiv \frac{\langle p_\infty \rangle - \langle p_{-\infty} \rangle}{\rho_{-\infty} U^2/2} = -\frac{2\sigma_T}{\beta^2}\left(\frac{2}{1-h^2}\int_h^1 \eta\, d\eta\, \frac{\Gamma(\eta)}{UL_T}\right) \equiv \frac{-2\sigma_T}{\beta^2}\,\frac{\bar{\Gamma}}{UL_T} \qquad (1)$$

where $\eta \equiv r/r_T = \sigma/\sigma_T$, $h = r_H/r_T$, $< >$ denotes the azimuthal average of a given quantity, $\beta^2 \equiv 1 - U^2/a^2 \equiv 1 - M^2$, and $L_T \equiv 2\pi r_T/B$, the blade spacing. The subscripts T and H denote tip and hub, respectively. The sign convention on Γ is such that it is negative for lifting blades. The corresponding torque required, to first order, is

$$T^{(1)} = -\rho_{-\infty} U^2 r_T^2 B \int_h^1 \eta\, d\eta \Gamma \qquad (2)$$

By extending these calculations consistently to second order (a procedure analogous to the computation of induced drag and wave drag in ordinary wing theory), the losses due to energy stored in the wakes of shed vorticity (when $\Gamma(r) \neq$ constant) as well as those due to acoustic radiation (for supersonic relative tip Mach numbers) were estimated. These are presented in figure 2 for a typical rotor ($B=40$, $h=0.8$), in terms of a dimensionless efficiency decrement. Since these results are essentially "integral relationships" (i.e., obtained from momentum balances, etc.) we expect them to carry over without change to the lifting surface theory, which will be the main subject of our discussion. Despite the linearizing assumptions inherent to the theory, we estimate that these results will be accurate up to static pressure ratios across the (single) rotor of about 1.3 (see eq. (1)). It should be noted that the "concentrated bound vortex solution" of reference 9 is *not* a lifting-line theory in the sense of Prandtl, since no quasi-two-dimensional assumptions were used.

The lifting *surface* theory, in analogy to the procedures described in reference 1, can be constructed from the concentrated bound vortex solution by distributing the bound vorticity, with its associated wakes, over helical surfaces representing the blades. Details will be made available shortly in reference 10. In the next sections, we describe the salient features of the theory and some of its more interesting results.

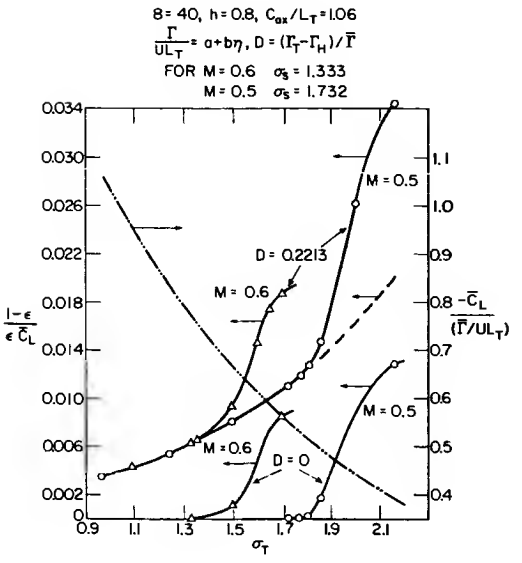

FIGURE 2.—*Losses for a typical rotor configuration as caused by (1) energy stored in wakes* ($D \neq 0$) *and (2) acoustic radiation* ($\sigma_T > \sigma_s$). *Solid lines (left-hand scale) give values of the efficiency decrement, normalized to* $\bar{C}_L$, *an average (over the span) sectional lift coefficient. The relation between* $\bar{C}_L$ *and* $\bar{\Gamma}$, *defined in the text, is shown, for this rotor geometry, by the broken line (right-hand scale). The sharp increase in losses due to acoustic radiation as* σ_T *exceeds* σ_s *is readily observable for both* $D = 0$ *and* $D = 0.2213$. *In the latter case, the efficiency decrement associated with nonuniform loading is comparable to the acoustic radiation loss. (Figure taken from ref. 9.)*

LIFTING SURFACE THEORY

The velocity potential obtained by distributing bound vorticity, in the manner described, over the helical surfaces representing the rotor blades can be written

$$\phi(x,\theta,r) = \frac{B}{2\pi\beta^2}\left(\int_0^{\hat{x}} \delta\phi^d \, d\xi + \int_{\hat{x}}^{c_{ax}^{(max)}} \delta\phi^u \, d\xi\right) \tag{3}$$

where ξ labels the *axial* location of the bound vortex filaments while

$$\hat{x} \equiv x \qquad 0 \leq x \leq c_{ax}^{(max)}$$

$$\hat{x} \equiv 0 \qquad x \leq 0$$

$$\hat{x} \equiv c_{ax}^{(max)} \qquad x \geq c_{ax}^{(max)}$$

If we denote by $\varphi(r) \equiv \tan^{-1}\sigma = \tan^{-1}(\omega r/U)$ the complement of the stagger angle at each radius, the axial projection of the local chord is $c_{ax}(r) = c\cos\varphi$, and in (3) $c_{ax}^{(max)}$ is the maximum of this quantity along the span. The elemental potentials $\delta\phi^u$ and $\delta\phi^d$ are, respectively, the upstream and downstream velocity potentials associated with B radial strips of concentrated bound vorticity located on the helical surfaces $x = \xi$, $\theta = \omega\xi/U + l\pi/B$, $l = \pm 1, \pm 3, \pm 5, \ldots$. Each strip has elementary chord $d\xi/\cos\varphi$ and strength $\gamma(\eta,\xi)\, d\xi/\cos\varphi$. Their associated wakes of free vorticity, proportional to $\partial/\partial\eta(\gamma/\cos\varphi)$, are included in $\delta\phi^d$. The

total bound vorticity (per blade) at each radial station is the local blade circulation:

$$\Gamma(r) = \Gamma(\eta r_T) = \int_0^{c_{ax}(r)} \gamma(\eta,\xi)\, d\xi/\cos\varphi \tag{4}$$

The elemental potentials occurring in (3) can be expressed as follows (ref. 10; real part implied)

$$\begin{aligned}\delta\phi^u(z,\theta,\sigma;\xi) = &-\sum_{k=1}^{\infty} \frac{\gamma_{0k}(\xi)}{2\lambda_{0k}} \exp\left[\lambda_{0k}\left(z-\frac{\omega\xi}{U}\right)\right] R_0\left(\kappa_{0k}\frac{\sigma}{\sigma_T}\right)\\ &+\sum_{n=1}^{\infty}\sum_{k=1}^{\infty}\left\{(-1)^n\frac{h_{nk}(\xi)}{\lambda_{nk}}+i\frac{\beta^2(-1)^n}{nB}\left[h_{nk}(\xi)+\gamma_{nk}(\xi)\right]\right\}\\ &\times\exp\left[inB\left(\theta-\frac{\omega\xi}{U}\right)\right]\\ &\times\exp\left[\left(\frac{inBM^2}{\beta^2}+\lambda_{nk}\right)\left(z-\frac{\omega\xi}{U}\right)\right] R_{nB}\left(\kappa_{nk}\frac{\sigma}{\sigma_T}\right)\end{aligned} \tag{5}$$

$$\begin{aligned}\delta\phi^d(z,\theta,\sigma;\xi) = &\bar{\gamma}(\xi)\left(z-\frac{\omega\xi}{U}\right)+\beta^2\frac{\gamma(\eta,\xi)}{\cos\varphi(\sigma)}\zeta_l\\ &+\sum_{n=1}^{\infty}\frac{2i\beta^2}{nB}(-1)^n\chi_n(\eta,\xi)\exp(inB\zeta)\\ &-\sum_{k=1}^{\infty}\frac{\gamma_{0k}(\xi)}{2\lambda_{0k}}\exp\left[-\lambda_{0k}\left(z-\frac{\omega\xi}{U}\right)\right] R_0\left(\kappa_{0k}\frac{\sigma}{\sigma_T}\right)\\ &+\sum_{n=1}^{\infty}\sum_{k=1}^{\infty}\left\{\frac{(-1)^n h_{nk}(\xi)}{\lambda_{nk}}-i\beta^2\frac{(-1)^n}{nB}\left[h_{nk}(\xi)+\gamma_{nk}(\xi)\right]\right\}\\ &\times\exp\left[inB\left(\theta-\frac{\omega\xi}{U}\right)\right]\\ &\times\exp\left[\left(\frac{inBM^2}{\beta^2}-\lambda_{nk}\right)\left(z-\frac{\omega\xi}{U}\right)\right] R_{nB}\left(\kappa_{nk}\frac{\sigma}{\sigma_T}\right)\end{aligned} \tag{6}$$

In these expressions, the "radial eigenfunctions" $R_{nB}(\kappa_{nk}\sigma/\sigma_T) \equiv R_{nB}(\kappa_{nk}\eta)$ are orthonormal combinations of Bessel and Neumann functions whose

properties, including the radial eigenvalues κ_{nk}, are determined by the requirement of vanishing radial velocity at hub and shroud. Details are available in references 1 and 3. The quantities λ_{nk}, determining the *axial* behavior of the acoustic modes, are given by

$$\left.\begin{aligned}\lambda_{nk}&=\frac{nB}{\beta\sigma_T}\sqrt{\frac{\kappa_{nk}^2}{n^2B^2}-\frac{\sigma_T^2M^2}{\beta^2}}\\ \lambda_{0k}&=\frac{\kappa_{0k}}{\beta\sigma_T}\end{aligned}\right\}\tag{7}$$

These quantities are either pure real (yielding axial decay) or pure imaginary (yielding propagating, "spinning" modes). Since the κ_{nk} are all greater than $|nB|$ (ref. 11), the latter possibility occurs only if $\sigma_T>M/\beta=\omega r_s/U$, and then only for a finite number of modes at each n; $k=1,2,\ldots k_n{}^*$. The condition $\sigma_T>\sigma_s$ implies supersonic relative Mach numbers at the tip.

In (6), the variable $\zeta\equiv\theta-\omega x/U=\theta-z$ is the helical coordinate used by Reissner (ref. 5) and the (generalized) function ζ_l is a "sawtooth function," the essential properties of which are that $\partial\zeta_l/\partial\theta=1$, $\partial\zeta_l/\partial z=-1$ *everywhere*, while the function itself is discontinuous (by an amount $\mp2\pi/B$) at $\zeta=\pm\pi/B$, $\pm3\pi/B$, ... The combination of the second and third terms in (6) makes up the wake potential mentioned earlier, representing the free vorticity shed in the wakes and the induced flow between them. The wake functions, $\chi_n(\eta,\xi)$, can be written in terms of modified Bessel functions of the first and second kind:

$$\begin{aligned}\chi_n(\eta,\xi)\equiv\chi_{nB}(nB\eta\sigma_T,\xi)&=\alpha_n(\xi)I_{nB}(nB\sigma)+\beta_n(\xi)K_{nB}(nB\sigma)\\ &+I_{nB}(nB\sigma)\int_{\sigma_H}^{\sigma}\frac{d}{d\sigma'}K_{nB}(nB\sigma')\sigma'\frac{\partial}{\partial\sigma'}\left[\frac{\gamma(\sigma'/\sigma_T,\xi)}{\cos\varphi(\sigma')}\right]d\sigma'\\ &-K_{nB}(nB\sigma)\int_{\sigma_H}^{\sigma}\frac{d}{d\sigma'}I_{nB}(nB\sigma')\sigma'\frac{\partial}{\partial\sigma'}\left[\frac{\gamma(\sigma'/\sigma_T,\xi)}{\cos\varphi(\sigma')}\right]d\sigma'\end{aligned}\tag{8}$$

where $\alpha_n(\xi)$ and $\beta_n(\xi)$ involve definite (radial) integrals over $\partial/\partial\sigma[\gamma(\eta,\xi)/\cos\varphi]$ and depend on the parameters σ_H and σ_T, as well as nB (refs. 3, 5, 9, and 10). Note that each $\chi_n(\eta,\xi)$ vanishes when $\gamma/\cos\varphi$ is independent of σ (or η); i.e., when $\Gamma=$ constant.

The quantities $\bar{\gamma}(\xi)$, $\gamma_{nk}(\xi)$ and $h_{nk}(\xi)$ are the coefficients of expansions of the functions $\gamma(\eta,\xi)/\cos\varphi$ and $\chi_n(\eta,\xi)$ in terms of the orthonormal radial functions $R_{nB}(\kappa_{nk}\eta)$. Thus,

$$\left.\begin{aligned}
\frac{\gamma(\eta,\xi)}{\cos\varphi(\eta\sigma_T)} &= \bar{\gamma}(\xi) + \sum_{k=1}^{\infty}\gamma_{0k}(\xi)\,R_0(\kappa_{0k}\eta) \\
\frac{\gamma(\eta,\xi)}{\cos\varphi(\eta\sigma_T)} &= \sum_{k=1}^{\infty}\gamma_{nk}(\xi)R_{nB}(\kappa_{nk}\eta); \quad n>0 \\
\chi_n(\eta,\xi) &= \sum_{k=1}^{\infty}h_{nk}(\xi)\,R_{nB}(\kappa_{nk}\eta)
\end{aligned}\right\} \tag{9}$$

The usual Fourier-Bessel formulas for the expansion coefficients apply; for example

$$\gamma_{nk}(\xi) = \int_h^1 \eta\,d\eta\,\frac{\gamma(\eta,\xi)}{\cos\varphi(\eta\sigma_T)}\,R_{nB}(\kappa_{nk}\eta)$$

while

$$\bar{\gamma}(\xi) = \frac{2}{1-h^2}\int_h^1 \eta\,d\eta\,\frac{\gamma(\eta,\xi)}{\cos\varphi} \tag{10}$$

Note that

$$\int_0^{c_{ax}^{(max)}} d\xi\bar{\gamma}(\xi) = \bar{\Gamma}$$

as defined in equation (1), and that the coefficients $\gamma_{0k}(\xi)$, as well as the $h_{nk}(\xi)$ vanish whenever $\gamma/\cos\varphi$ is independent of radius.

In the special case for which $c_{ax}=$constant and $\gamma(\eta,\xi)/\cos\varphi$ is factorizable (i.e., $\gamma/\cos\varphi=\Gamma(\eta)g(\xi)$) we have the especially simple relationships, $\gamma_{nk}(\xi)=\Gamma_{nk}g(\xi)$, $h_{nk}(\xi)=H_{nk}g(\xi)$, $\bar{\gamma}(\xi)=\bar{\Gamma}g(\xi)$, where, from (4),

$$\int_0^{c_{ax}} g(\xi)\,d\xi = 1 \tag{11}$$

Γ_{nk}, H_{nk} and $\bar{\Gamma}$ are then identical to the corresponding quantities occurring in the concentrated bound vortex solution (refs. 9 and 10), in which the blades are characterized by $\Gamma(r)$.

The three-dimensional lifting surface solution, described formally by equations (3) through (10), has the desired property of producing discontinuities (at the helical surfaces representing the blades) of the velocity component parallel to the blade surface. In fact, if we denote this component by $v_{x'}$, the discontinuity in $v_{x'}$ is $-\gamma(\eta,x)$, and the blade loading is $-\rho_{-\infty}U_r\gamma(\eta,x)$, where $U_r\equiv(U^2+\omega^2r^2)^{1/2}$. The detailed proof that (3) with (5) and (6) has this property is available in reference 10. At the same time $v_{y'}$, the velocity component perpendicular to the helix of advance, is *continuous*, and $v_{y'}/U_r$ defines the slope of the blade camber

line (in the absence of thickness effects) for any loading. As is usual in wing theory, if the blade shape is specified and the loading required, the mathematical problem becomes one of inverting an integral equation—in our case an unusually complicated one.

Actually, if one is given a shape for the rotor blades (desired thickness and camber), the thickness problem must be solved first (refs. 1 and 2) since the distribution of sources used to obtain the desired thickness distribution inevitably produces a camber distribution of its own. This "camber due to thickness" must then be included in the distributed vortex problem if one is to obtain the desired overall camber.

The results given in this paper, however, will be restricted to those for the indirect lifting problem: given the loading, and omitting thickness effects, what is the associated camber line of the blades, how does the flow and pressure field develop, and what is the performance of the rotor? The last of these questions has been substantially answered in reference 9, since most performance characteristics calculable in this theory do not depend on the details of the chordwise loading distribution but primarily on $\Gamma(r)$. This is not to say that the chordwise loading distribution is not important; for example, it will affect boundary-layer behavior, stall margins, etc., of the rotor and is of great interest for these and other reasons.

RELATION TO AXISYMMETRIC "THROUGH-FLOW" THEORY

Let us consider first the mean pressure level (i.e., the azimuthal average pressure) developed by the rotor. We have generally, in the strictly linear approximation,

$$\tilde{p} \equiv p - \langle p_{-\infty} \rangle = -\rho_{-\infty} U \sqrt{1+\sigma^2} v_{x'} \tag{12}$$

where

$$\begin{aligned} v_{x'} &= v_x \cos \varphi + v_\theta \sin \varphi \\ &= \frac{\omega}{U\sqrt{1+\sigma^2}} \left(\frac{\partial \phi}{\partial z} + \frac{\partial \phi}{\partial \theta} \right) \end{aligned} \tag{13}$$

Then for any axial station downstream of the rotor $x > c_{ax}^{(max)}$, using (3)–(6) and averaging over θ, we obtain

$$\langle p(x,r) \rangle^d - \langle p_{-\infty} \rangle$$

$$= -\omega \rho_{-\infty} \left\langle \frac{\partial \phi}{\partial z} + \frac{\partial \phi}{\partial \theta} \right\rangle$$

$$= -\rho_{-\infty}\frac{\omega B}{2\pi\beta^2}\left\{\bar{\Gamma}+\frac{1}{2}\sum_{k=1}^{\infty}\int_0^{c_{ax}^{(max)}} d\xi \exp\left[-\lambda_{0k}\left(z-\frac{\omega\xi}{U}\right)\right]\gamma_{0k}(\xi)R_0(\kappa_{0k}\eta)\right\} \tag{14}$$

Upstream of the rotor ($x<0$) the corresponding result is

$$\langle p(x,r)\rangle^u - \langle p_{-\infty}\rangle = \rho_{-\infty}\frac{\omega B}{4\pi\beta^2}\sum_{k=1}^{\infty}\int_0^{c_{ax}^{(max)}} d\xi \exp\left[\lambda_{0k}\left(z-\frac{\omega\xi}{U}\right)\right]R_0(\kappa_{0k}\eta)\gamma_{0k}(\xi) \tag{15}$$

If we recall that all γ_{0k}'s are zero when $\gamma/\cos\varphi$ is independent of η (implying "constant work" design, $\Gamma=\text{constant}=\bar{\Gamma}$), we see from (15) that for a constant work rotor, there is no change in *mean* pressure (starting from upstream) until the rotor itself is reached, while from (14) we see, for the same design, that the entire mean static pressure rise is achieved within the rotor passage and the "far-field" value (compare eqs. (14) and (11)) is already attained at $x=c_{ax}^{(max)}$.

On the other hand, if $\Gamma(r)\neq$constant, then the γ_{0k}'s do *not* vanish and there is essentially *exponential* approach, away from the rotor, to the respective upstream and downstream values of the mean pressure level. This type of result is typical of axisymmetric theories of axial compressor flows (ref. 12), but the rate of approach is, of course, sensitive to the assumed area distribution of the flow annulus (ref. 13). For the particular case we have considered ($r_H/r_T=\text{constant}$), the "decay length" for approach to the upstream and downstream values is of order $\beta(r_T-r_H)/\pi$ (see eq. (7) and refs. 11 and 12). At large (subsonic) axial Mach numbers, approach to the asymptotic states is very rapid, as expected (ref. 12).

The result (1) or (14) indicates a constant radial static pressure profile far downstream of the rotor, at obvious variance with the need for a radial pressure gradient to balance the centripetal acceleration associated with the induced tangential velocities (see eq. (18)). This is simply a result of the linearization used throughout the present theory (for example, eq. (12)). However, comparisons between appropriate azimuthal averages of the results from the present three-dimensional (but linear) theory and higher-order (but two-dimensional) "actuator disc" results are expected to suggest means of identifying and including the more important nonlinear effects. We have already shown (ref. 9) that the second-order calculations, used in that paper to compute losses, are consistent with "radial equilibrium". It should be possible to include certain nonlinear effects, such as centrifugal effects, consistently in a modified three-dimensional theory. Further work in this direction is underway.

The results (14) and (15) can be understood in terms of the mean (azimuthally averaged) stream-surface deflections associated with non-uniform loading. (Note that the wake functions themselves, depending

only on ζ and η, yield zero first-order pressure perturbations.) If $\Gamma(r)$ increases from hub to tip, more work is done by the rotor at the tip than at the hub. This appears initially (just behind the rotor) as a higher pressure near the tip than at the hub. In fact, using (7) and evaluating (14) for $x \approx c_{ax}^{(max)}$ with the assumption $c_{ax}^{(max)}/r_T \ll 1$, we find, immediately behind the rotor,

$$\langle p(c_{ax},r)\rangle^d - \langle p_{-\infty}\rangle \cong -\rho_{-\infty}\frac{\omega B}{4\pi\beta^2}\left(\Gamma(\eta)+\bar{\Gamma}\right) \tag{16}$$

where we have used the first of equation (9) and also equation (4). The higher (lower) pressure at the tip (hub) must relax to the constant value given by the linear theory far downstream of the rotor. Moreover, the azimuthally averaged flow is effectively subsonic if $M<1$ (ref. 12). This means contraction of the outermost streamtubes and expansion of those near the hub. The stream surfaces must, therefore, be deflected outwards. In fact, we find

$$\delta(\eta)_{\langle\psi\rangle=\text{const}} \cong \frac{\sigma_T \bar{\Gamma}}{UL_T\eta}\int_h^\eta \eta\, d\eta\left(1-\frac{\Gamma}{\bar{\Gamma}}\right) \tag{17}$$

provided $\Gamma - \bar{\Gamma} \ll \bar{\Gamma}$. These average radial stream-surface deflections are zero, as required, at $\eta = h$ and $\eta = 1$ and are positive if Γ increases radially and negative if Γ decreases radially. There is no (average) streamline deflection if $\Gamma = \text{constant} = \bar{\Gamma}$.

Associated with (14), (15), and (17) are certain azimuthally averaged tangential, axial, and radial velocity profiles. Downstream of the rotor (see also ref. 9), these are given by

$$\langle v_\theta\rangle^d = \frac{B\Gamma(\eta)}{2\pi r} \tag{18}$$

$$\langle v_x\rangle^d = \frac{\omega B}{2\pi U\beta^2}\left\{\bar{\Gamma} - \beta^2\Gamma(\eta) + \frac{1}{2}\sum_{k=1}^{\infty}\int_0^{c_{ax}^{(max)}} d\xi \exp\left[-\lambda_{0k}\left(z-\frac{\omega\xi}{U}\right)\right]\gamma_{0k}(\xi)R_0(\kappa_{0k}\eta)\right\} + U \tag{19}$$

$$\langle v_r\rangle^d = \frac{-\omega B}{4\pi\beta U}\sum_{k=1}^{\infty}\int_0^{c_{ax}^{(max)}} d\xi \exp\left[-\lambda_{0k}\left(z-\frac{\omega\xi}{U}\right)\right]\gamma_{0k}(\xi)R_0'(\kappa_{0k}\eta) \tag{20}$$

The actual velocity field derivable from (3)–(6), of course, is curl-free except at the B helical sheets (wakes) of concentrated shed vorticity, this vorticity having strength proportional to $d\Gamma/d\eta$ and being oriented so as to lie in the helical sheets representing the wakes.

By contrast, the vorticity of the (mean) downstream velocity field defined by (18)–(20) is

$$\Omega^{\langle v\rangle} \equiv \text{curl } \langle v\rangle^d = \frac{\Gamma'(\eta)}{L_T r}\left(1, \frac{\omega r}{U}, 0\right) \tag{21}$$

Thus, since $\Omega_\theta^{\langle v\rangle}/\Omega_x^{\langle v\rangle} = \omega r/U$, an important effect of defining an "equivalent axisymmetric" flow (through averaging the more detailed three-dimensional theory) is to replace the original concentrated vorticity by an equal total amount of vorticity which is, however, distributed uniformly over the flow annulus, yet still oriented along the zeroth-order streamlines. This distributed downstream vorticity is an important feature of axisymmetric through-flow theories (ref. 12); results such as (21), (19) and (14) help to establish connection between the latter theories and that described here.

It should be clear from the preceding that the three-dimensional (but linearized) potential theory contains many important elements of the axisymmetric theories and has, in addition, the capacity to describe azimuthal variations superposed on those results. Some interesting examples of the latter are given in the following section.

THREE-DIMENSIONAL PRESSURE FIELD (LIFTING PROBLEM)

The azimuthally-averaged pressure fields (14) and (15) are the same, regardless of whether the compressor is transonic or not (ref. 12). But the azimuthal *variations* about these mean levels are vastly different, depending on (1) whether or not the tip relative Mach number is supersonic and (2) whether or not the rotor is uniformly loaded (along the blade span).

The latter observation comes from consideration of the conditions under which transonic "acoustic resonance" (see the introduction) can occur for the strictly lifting problem. As mentioned earlier, when $M_{rT}^2 \equiv M^2(1+\sigma_T^2) > 1$, some of the quantities λ_{nk} (eq. (7)), as determined by the linear inviscid theory, can vanish. A glance at equations (5) and (6) shows that when this happens some of the acoustic eigenmodes can be amplified indefinitely unless the corresponding $h_{nk}(\xi)$ are identically zero. This is the "resonance" to which we have referred. However, we have already noted that the $h_{nk}(\xi)$ are, in fact, zero if the spanwise loading is constant at each ξ. Thus a constant work rotor with similar chordwise loading profiles (i.e., $\gamma(\eta,\xi)/\cos\varphi = \bar{\Gamma} g(\xi)$) excites no transonic resonance. A more general way of saying this is that any (purely lifting) transonic rotor which sheds wakes of free vorticity can excite acoustic resonances of spinning modes and otherwise not. (Finite values of h_{nk}

can be regarded as representing excitation of acoustic modes by the wakes.) Of course, the finite thickness of the blade of any real rotor will always induce transonic resonances (ref. 2).

If transonic resonance is excited, one or several acoustic modes will be singled out and tend to dominate the pressure field, although the (linear) azimuthal average of the pressure fields will vanish. Naturally, the resonant modes do not attain infinite amplitudes; their finite amplitudes are easily predicted by including either viscous effects (as in refs. 1 and 2) or certain nonlinear effects (as in ref. 10) or both. In the following, we present typical numerical results extracted from reference 10; included are pressure-field results for a typical rotor ($B=40$, $h=0.8$) operating both subsonically ($M_{rT}=0.9$) and transonically ($M_{rT}=1.054$). In reference 10, both a uniformly loaded rotor ($\Gamma=\bar{\Gamma}$) and a rotor with linearly increasing $\Gamma(\eta)$, characterized by an increase of approximately 20 percent in Γ from hub to tip, were analyzed. However, for lack of space we present here only the results for a uniformly loaded rotor. The axial Mach number in the examples discussed is $M=0.5$. The specific loading distributions used in the calculations were of the factorizable type $\gamma/\cos\varphi=\Gamma(\eta)g(\xi)$, where

$$g(\xi)=\frac{8}{\pi c_{ax}^2}\sqrt{\xi(c_{ax}-\xi)}$$

Note that this chordwise loading distribution is symmetric about the midchord, nonsingular, and satisfies the Kutta condition and the normalization (11).

Our first example (fig. 3) shows the "near field" subsonic upstream pressure fluctuation, at $x/c_{ax}=-0.1$, over an azimuthal period $\Delta\theta=2\pi/B$ (corresponding to a single blade passage). Five radial stations are indicated. The tip Mach number being 0.9, we have $\sigma_T=1.46$. The pressure side of the airfoil corresponds to the smaller values of $B\theta/2\pi$. For the solidity noted in figure 3, the projection of the helix of advance forward from $x=0$ (for which $B\theta/2\pi=\frac{1}{2}$ is the blade leading edge) to $x/c_{ax}=-0.1$ corresponds to $B\theta/2\pi=0.35$. Note that the high- and low-pressure regions remain relatively well identified just upstream of the airfoil (typical of subsonic flow). The fluctuating signal is superposed on a zero mean pressure level, in agreement with (15) for a uniformly loaded rotor. This pressure signal is almost entirely dominated here by the ($n=1$, $k=1$) eigenmode, not because of any resonance effect, but because the exponential decay of this mode (for $B=40$) is significantly slower than that of the remaining modes.

Let us contrast this behavior (fig. 4) with the same rotor of the same solidity, but at the transonic state of $M_{rT}=1.054$. In this case, $\sigma_T=1.84$, and the angle ($B\theta/2\pi$) of projection of the leading edge is approximately 0.3. The fluctuating pressure signal is significantly distorted, relative to

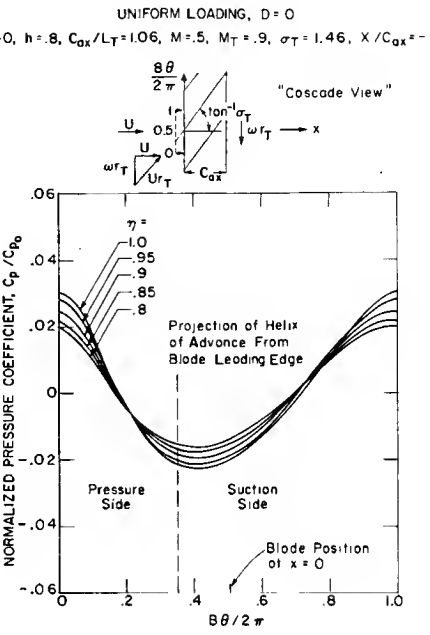

FIGURE 3.—*Pressure variation just upstream of typical uniformly loaded rotor operating at* subsonic *tip Mach numbers. Angular range corresponds to one full blade passage.*

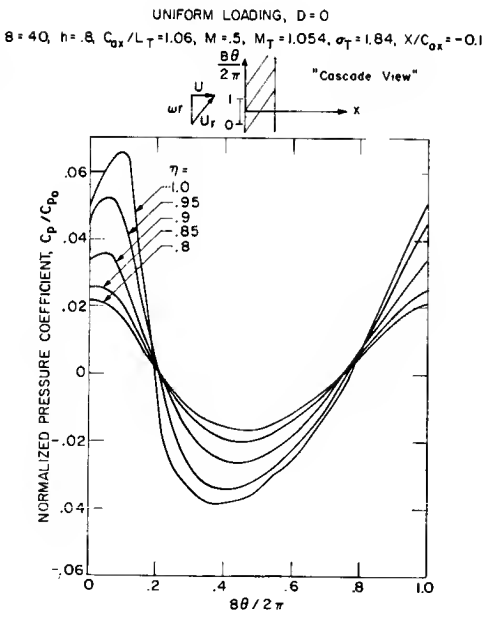

FIGURE 4.—*Pressure variation just upstream of typical uniformly loaded rotor operating at* supersonic *tip Mach numbers. Note distortion due to modes above cut-off.*

the subsonic case, by the presence of a large number of modes which are now above cut-off and therefore propagate. (For example, the $k = 1$ modes for all n are above cut-off at this tip Mach number; the (7,2) mode is also

above cut-off, etc.) The shift toward smaller angles of the expansion region just ahead of the blade is consistent with the expected formation (for the specified loading) of an expansion fan emanating from the leading edge of the blade tip ($\eta = 1$), but the flow field is still predominantly subsonic in character over the whole annulus. Hence, no really clear-cut development of a quasi-two-dimensional type flow field can be identified in this region.

A clearer distinction between hub and tip section contributions to the pressure pattern seems to develop just behind the rotor (figure 5) indicating some semblance of quasi-two-dimensional behavior. Here, the pressure signal oscillates about the uniform downstream level given by (1) or (14) at each η (because of the uniform loading) but a fairly strong local compression followed by an equally strong expansion fan seems to be emanating from the aft portions of the blade tips.

The results available in reference 10 indicate similar behavior for the nonuniformly loaded rotor, except that the near-field upstream and downstream pressure signals oscillate about different mean levels for each η, in accord with (15) and (14). One other major difference occurs for the case of nonuniform Γ, however; namely, the expected transonic resonance appears (see earlier discussion). For $M_{rT} = 1.054$ the (1,1) mode is the one nearest resonance, and the relative fluctuations in the near-field pressure that it produces are noticeably larger than for the constant-Γ case. The radial structure of this resonant mode also makes it more difficult to separate hub and tip behavior in the strip theory sense.

Far-field pressure signals (for example, at $x/c_{ax} = -5.0$, $x/c_{ax} = +6.0$) were also computed in the work reported in reference 10. As expected, essentially no pressure fluctuation about the azimuthal mean is observed

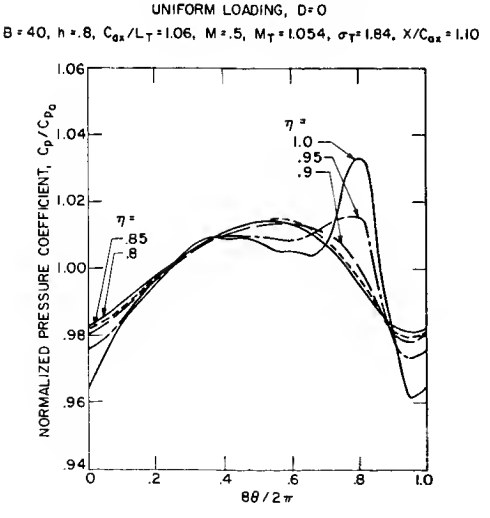

FIGURE 5.—*Pressure variation just* downstream *of the same rotor as in figure 4. Note development of a semblance of a quasi-two-dimensional pattern.*

at subsonic tip Mach numbers, while substantial fluctuations, comparable to the near-field values, are found to be present as soon as M_{rT} exceeds unity.

CONCLUDING REMARKS

In this paper, we have discussed some of the aspects of the three-dimensional aerodynamic theory of an axial compressor rotor. Our main emphasis has been on the newly developed lifting-surface (distributed-vortex) theory which forms the complement to the previously developed (distributed-source) theory for blade thickness effects.

In the third section, we showed that the present theory contains many aspects of the axisymmetric through-flow or actuator-disc theories, while in the fourth section we gave examples of the type of additional information that the three-dimensional theory offers.

It may be recalled that in reference 1 the relationship between three-dimensional and quasi-two-dimensional cascade theory was emphasized. Not surprisingly, in the lifting problem just as in the thickness problem, cascade theory, and corrections to it, can be derived readily from the three-dimensional theory. The techniques involved are similar to those in reference 1; details and some examples are available in reference 10.

We find, in short, for the purely lifting case, that quasi-two-dimensional cascade theory is an excellent approximation, at least within and near the blade passage, for uniformly loaded rotors, even in the transonic regime. However, for a rotor with only moderate variations in spanwise loading, we find that the wake-induced velocities have a surprisingly large effect on the effective incidence of the blades. Much work remains to be done, therefore, before the complete relationship between cascade theories (and/or data) and the aerodynamics of three-dimensional compressor rotors will be fully understood. Our expectation is that the present theory, despite the limitations imposed by our assumption of small disturbances, neglect of viscosity, etc., will be a useful key in relating all the various approximate theories to the full three-dimensional problem. It has pieces of each part of the puzzle.

REFERENCES

1. McCune, J. E., *J. Aerospace Sci.*, Vol. 25, No. 9, 1958, p. 544.
2. McCune, J. E., *J. Aerospace Sci.*, Vol. 25, No. 10, 1958, p. 616.
3. Okurounmu, O., *Wave Drag in Transonic Axial Compressors*. Sc.D. dissertation, M.I.T., November 1967.
4. Davidson, R. E. *Linearized Potential Theory of Propeller Induction in a Compressible Flow*. NACA TN 2983, 1953.
5. Reissner, H., *J. Aeron. Sci.*, Vol. 5, No. 1, 1937, p. 1.

6. Tyler, J. M., and T. G. Sofrin, preprint 345 D, SAE Aeronautic Meeting, 1961; Morfey, C. L., *J. Sound Vib.*, Vol. 1, No. 60, 1964; Slutsky, S., AFOSR-UTIAS Symposium on Aerodynamic Noise (Toronto), May 1958.
7. Morse, P. M., and K. U. Ingard, *Theoretical Acoustics*. McGraw-Hill Book Co., Inc. (New York), 1968.
8. Sparis, P., and D. Oliver, private communication. Nonlinear numerical studies, currently underway, of sheared flow past a nonlifting wing in a rectangular duct, with the inflow Mach number varying from subsonic to supersonic along the wing span, indicate similar effects at the "subsonic" sections.
9. Okurounmu, O., and J. E. McCune, Three-Dimensional Vortex Theory of Axial Compressor Blade Rows at Subsonic and Transonic Speeds. To be published, *AIAA J.*, 1970.
10. Okurounmu, O., and J. E. McCune, *Transonic Lifting Surface Theory of Axial Flow Compressors*. To be published as United Aircraft Research Laboratories Report, East Hartford, Connecticut, 1970.
11. Watson, G. N., *A Treatise on the Theory of Bessel Functions*. Second Ed., Mac Millan, 1944.
12. Marble, F. E., Three-Dimensional Flow in Turbomachines. Princeton Series on *High Speed Aerodynamics and Jet Propulsion*, Vol. 10, Sec. C, Princeton U. Press, 1964, pp. 83–166.
13. Oates, G. C., *Theory of Throughflow in Axial Turbomachines With Variable Wall Geometry*. AFOSR TN 59–680, August 1959.

DISCUSSION

J. C. VRANA (McGill University): Do you find that, as blade number is increased, the 3-dimensional solutions converge toward the infinitely bladed 2-dimensional approximations, regardless of circulation distribution? Going now in the opposite direction (as I have been mostly involved with low aspect ratios) would you agree that below a certain number of blades (10 to 12) it becomes impossible to design them for a prescribed variation of circulation (say 20 percent variation in circulation from mean)?

McCUNE (author): With regard to the first question, the 3-dimensional solutions converge, provided you are not in the transonic regime, to the 2-dimensional cascade solutions in the limit of large blade number and hub tip ratio approaching unity. This we showed for the thickness case in 1956 (refs. 1 and 2) and for the lifting case in reference 9 of the paper. On the other hand, for the "infinitely bladed" 2-dimensional approximation, by which I take it you mean the axisymmetric through-flow theory emphasized in the present paper, the 3-dimensional solutions will converge to *that* 2-dimensional approximation as $B \rightarrow \infty$, regardless of regime. These are, however, formal mathematical results; I believe that in almost any practical case 3-dimensional effects play a role.

Going in the other direction, the answer would have to depend on what you mean by "impossible". With *present* theory, insofar as it does not include induced velocity effects, I think it would be impossible to correctly design the blades, even for blade numbers as high as 40 or 80 (let alone 10 or 12), with 20 percent variation in circulation from mean. This is especially true in the transonic regime. While the theory presented in our paper is limited by the linearizing assumptions, it is intended as a step in the direction of making such design possible. We intend to pursue it. An important step is to include thickness effects (ref. 1) since they induce camber of themselves.